Application of CAD-Neutronics Coupling to Geometrically Complex Fusion Systems

M.E. Sawan, P.P.H. Wilson, T. Tautges, L.A. El-Guebaly, D.L. Henderson, T.D. Bohm, E.P. Marriott, B. Kiedrowski, B. Smith, A. Ibrahim, R. Slaybaugh

May 2009

UWFDM-1363

Prepared for the 23rd Symposium on Fusion Engineering (SOFE), May 31-June 5, 2009, San Diego CA.

FUSION TECHNOLOGY INSTITUTE

UNIVERSITY OF WISCONSIN

MADISON WISCONSIN

Application of CAD-Neutronics Coupling to Geometrically Complex Fusion Systems

M.E. Sawan, P.P.H. Wilson, T. Tautges, L.A. El-Guebaly,
D.L. Henderson, T.D. Bohm, E.P. Marriott, B. Kiedrowski,
B. Smith, A. Ibrahim, R. Slaybaugh

Fusion Technology Institute
University of Wisconsin
1500 Engineering Drive
Madison, WI 53706

http://fti.neep.wisc.edu

May 2009

UWFDM-1363

Prepared for the 23rd Symposium on Fusion Engineering (SOFE), May 31-June 5, 2009, San Diego CA.

Application of CAD-Neutronics Coupling to Geometrically Complex Fusion Systems

M.E. Sawan[1], P.P.H. Wilson[1], T. Tautges[2], L.A. El-Guebaly[1], D.L. Henderson[1], T.D. Bohm[1], E.P. Marriott[1], B. Kiedrowski[1], B. Smith[1], A. Ibrahim[1], R. Slaybaugh[1]
[1]Fusion Technology Institute, University of Wisconsin-Madison, Madison, WI 53706, sawan@engr.wisc.edu
[2] Argonne National Laboratory, Argonne, IL

Abstract— **An innovative computational tool (DAG-MCNP) has been developed for efficient and accurate 3-D nuclear analysis of geometrically complex fusion systems. Direct coupling with CAD models allows preserving the geometrical details, eliminating possible human error, and faster design iterations. DAG-MCNP has been applied to perform 3-D nuclear analysis for several fusion designs and demonstrated the ability to generate high-fidelity high-resolution results that significantly improve the design process. This tool will be the core for a full CAD-based simulation predictive capability that couples engineering analyses directly to the CAD solid model.**

Keywords- Monte Carlo, CAD models, 3-D nuclear analysis

I. Introduction

Fusion systems are geometrically complex requiring detailed three-dimensional (3-D) nuclear analysis to address tritium self-sufficiency, nuclear heating, radiation damage, shielding, and radiation streaming issues. In addition, engineering designs for components of fusion devices are dominated by computer-aided design (CAD) processes. Generating geometry input files manually for 3-D nuclear analyses can be a tedious and error-prone process. In an effort to automate this process, several tools were developed [1,2] to translate the CAD model into native MCNP [3] geometry input. This approach requires modification of the CAD model to eliminate or simplify complex high-order surfaces and may result in much greater number of cells. To facilitate performing 3-D nuclear analysis for geometrically complex systems, we developed an innovative computational tool, Direct Accelerated Geometry MCNP (DAG-MCNP), that performs the calculations directly in the CAD model [4,5]. This allows preserving the geometrical details without any simplification, eliminates possible human error in modeling the geometry, and allows faster design iterations. It also facilitates coupling to other engineering analysis codes by using common geometry. In this paper, a brief description of the computational approach used in DAG-MCNP is given.

DAG-MCNP has been successfully validated using an ITER benchmark problem [6]. The tool has been applied to 3-D nuclear analysis for several fusion designs including the ARIES Compact Stellarator (ARIES-CS) [7], the High Average Power Laser (HAPL) inertial fusion power plant [8], ITER first wall/shield (FWS) modules [9], and the ITER dual coolant lead lithium (DCLL) test blanket module (TBM) [10]. Highlights of these analyses are presented to demonstrate the capability of that tool in generating high-fidelity high-resolution results that provide great help to the design process of geometrically complex fusion systems with high degree of heterogeneity.

II. DAG-MCNP Computational Approach

The geometrical description native to Monte Carlo radiation transport codes, such as MCNP, relies on Boolean combinations of polynomial surfaces of second order or less. This requires extensive human effort that could introduce errors particularly as geometrical complexity increases. To alleviate this problem, several tools were developed to translate the CAD model into native MCNP geometry input [1,2]. This approach requires modification of the CAD model to eliminate or simplify complex high-order surfaces and often results in much greater number of cells than in the original CAD model. In DAG-MCNP [4,5], the CAD model is read and evaluated directly by the Monte Carlo code. This approach provides a number of advantages including the ability to represent surfaces beyond the limitations of the native MCNP geometry and the introduction of a common domain representation that facilitates coupling to other physics simulations.

The fundamental geometric operation in a Monte Carlo radiation transport code is to test the distance between a point and surface, along a particular ray. The DAG-MCNP approach uses the Mesh-Oriented datABase (MOAB) [11] and Common Geometry Module (CGM) [12] software libraries to provide this ray-surface intersection capability directly on the surfaces of the CAD-based solid model. The overwhelming majority of execution time in a direct geometry approach is the ray tracing used to track particles as they travel through and interact with the domain. Several methods have been developed to accelerate this calculation. Some of these methods involve the preparation of the geometric model, some the actual ray tracing process, and some the use of ray tracing in conjunction with radiation interactions with the domain. The most significant of these accelerations is to perform facet-based ray-tracing. The resulting code runs at speeds within a factor of 2-4 of the standard MCNP, with negligible loss of accuracy due to the facet-based model in typical cases. Reference [5] gives detailed description of these accelerations.

The workflow includes several steps. The initial step is to construct the geometrical model in a CAD-based system. It is essential to ensure that the model is “clean”, with each point in the space uniquely defined in a single volume. This might require some repair for overlapping volumes or to establish proper contact between adjacent volumes.

Another part of the geometry preparation is to perform the imprint and merge process to eliminate duplication of surfaces between adjacent volumes in the model [5]. The result is a series of contiguous volumes, separated from each other by surfaces each shared by two volumes, with remaining surfaces bounding a single volume, with void space on the other side. This makes finding the volume entered after crossing a surface a topological check, which is much more efficient than ray-tracing. One of the most complicated and tedious steps in preparing a geometry for analysis is the generation of the complement, or void-space, that surrounds all the solid/liquid objects in a model. CAD-based models do not explicitly include such spaces in the model. In the workflow of preparing a model for DAG-MCNP, this space must be created, generally by a sequence of Boolean operations between an enclosing volume and all the volumes that make up the solid model. Any complement defined explicitly this way is often very complex and convoluted. We developed an approach in which the complement is represented implicitly. The implicit complement capability is now a standard feature of DAG-MCNP [5].

Most features of the standard MCNP are now supported in DAG-MCNP. Important functionality enhancements have been implemented including support for the standard surface flux/fluence tally, support for reflecting boundary conditions, and correct implementation of the variance reduction techniques. The ability to use the surface source write/read capability is another important improvement facilitated by a fundamental improvement in the ability of DAG-MCNP to unambiguously define which cell a particle is in when it is on a boundary between cells [5]. In addition, the integration of the direct geometry capability with the MCNP software was improved, largely by providing a more robust mechanism for changing the standard input file from its standard format. This resulted in the ability to allocate materials with densities and define tallies, boundary conditions, and cell importances in the solid model geometry file itself, resulting in a reduced burden on the user.

III. VALIDATION USING ITER BENCHMARK

A CAD model based on a 40° sector of ITER has been developed for ITER neutronics benchmark calculations as shown in Fig. 1. The model includes all ITER components. Detailed structures in each component are suppressed and homogenized material definitions are used. The model is substantially simplified in comparison to the full detailed design drawings to allow using only 2nd-order surfaces required by the tools employing translation approach. Source neutrons were sampled from the exact ITER source profile. DAG-MCNP was compared to two translation-based approaches [1,2] on this ITER benchmark. While the DAG-MCNP approach used a CAD model which was close to the original model provided for the benchmark, the other approaches translated the CAD model into native MCNP geometry with each translation resulting in a different number of cells and surfaces. The results for neutron wall loading, divertor fluxes and heating, magnet heating, and mid-plane port shielding and streaming were compared [6]. Despite small variations in the results, the discrepancies are typically of a magnitude that will not be significant when other engineering uncertainties are included. It was concluded these tools are considered sufficiently mature for further use in the nuclear analysis of ITER and its components [6]. Timing results for the different approaches were also compared indicating that DAG-MCNP required only a factor of 1.5-2.5 more computing time compared to the translation approaches [5].

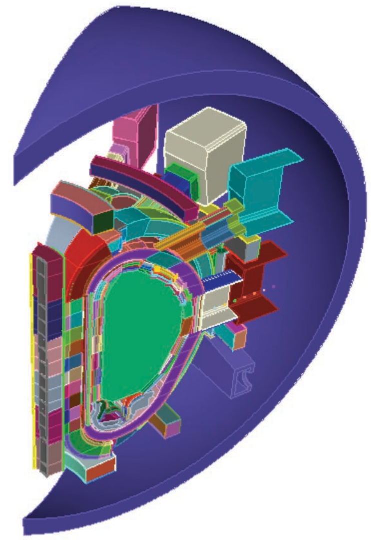

Figure 1. CAD model of the ITER benchmark problem.

IV. NUCLEAR ANALYSIS OF ITER FWS MODULES

The ITER first wall/shield (FWS) modules consist of a plasma facing first wall (FW) section followed by a shielding section [9]. These modules provide the main thermal and nuclear shielding for the vacuum vessel (VV) and external machine components. The FWS is segmented both in the poloidal and toroidal directions. Eighteen modules with different dimensions are arranged in the poloidal direction. While the design is going through iterations for enhanced performance, the general features include a FW panel assembly that consists of Be armor, Cu heat sink, and steel structure with embedded water coolant tubes. The shield module includes a front steel plate, a front water coolant manifold, a shielding zone with coaxial coolant channels, and a back shield plate. The design of the FWS modules includes assessment of the stresses due to nuclear heating and performing detailed computational fluid dynamics (CFD) and electromagnetic (EM) analyses. Accurate calculation of temperature distribution requires accurate knowledge of the volumetric nuclear heating due to neutrons and secondary gamma photons. In addition, re-welding is required at several locations in the FWS module and the VV behind it that requires accurate determination of helium production in the structural material. Therefore, detailed mapping of nuclear heating, radiation damage, and helium production is an essential input to the design process.

In order to capture the impact of the significant heterogeneity of the FWS module, we used DAG-MCNP to perform detailed nuclear analysis for several of the FWS design variations [13,14]. A detailed 3-D CAD model of an initial FWS module 13 design, shown in Fig. 2, was inserted into a 1-D radial approximation including homogenized representations of the inboard FWS, plasma, and vacuum vessel. This hybrid approach is used to improve overall computing efficiency while still resolving the influence of features in the analysis region [13]. A 14.1 MeV uniform source between the inboard and outboard side is used to simulate the ITER plasma. Results were normalized to a neutron wall loading for this module calculated in the 3-D ITER benchmark [6].

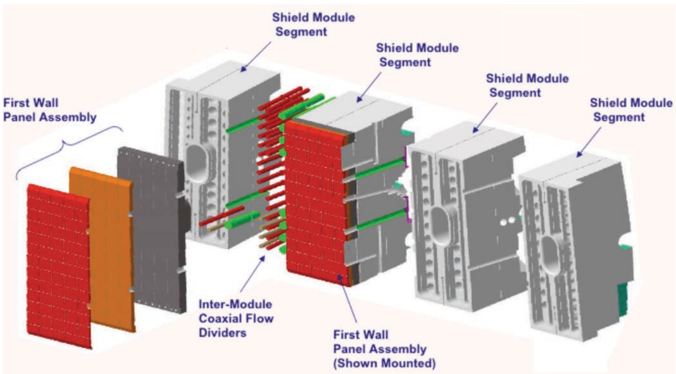

Figure 2. Elements of the FWS module.

Heating, radiation damage, and helium generation profiles through module 13 were determined using 0.5 cm x 0.5 cm x 1.0 cm mesh tallies. Fig. 3 provides a visualization of the nuclear heating throughout the front part of the FWS. It clearly shows the variation of nuclear heating due to geometrical changes and attenuation as one moves from the front of the FW deeper into the FWS module. Fig. 4 shows nuclear heating on a surface within the front reservoir. These high fidelity, high-resolution results revealed important heterogeneity effects on nuclear parameters [13]. While at a given radial location, nuclear heating is higher in steel than in water regions, peaking in steel nuclear heating occurs at the interface with water because of gamma generation in the water itself and the softer neutron spectrum in SS resulting in more gamma generation. He production results in the steel indicated peaking at the interface with water [13] that is attributed to a softer neutron spectrum resulting in increased He production primarily in B and Ni.

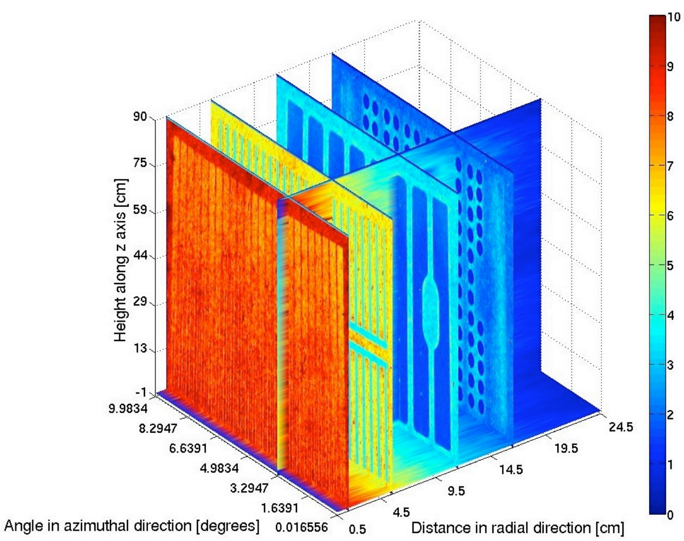

Figure 3. 3-D visualization of nuclear heating in FWS module.

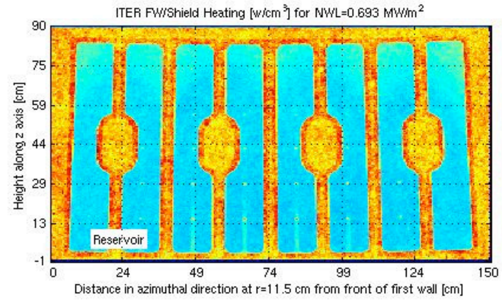

Figure 4. Nuclear heating distribution in the front reservior region.

In order to accurately represent the source profile in the plasma and account for secondary contribution from other components in the ITER plasma chamber, we utilized the surface source write/read feature in DAG-MCNP in the analysis for a recent FWS module design shown in Fig. 5. A surface source was written using the 3-D model of ITER with a detailed plasma source. During this simulation an approximation of the FWS module was used with 4 homogenized layers. The surface source was then used at the front surface of the detailed CAD model for the FWS module with reflecting boundaries on the sides. A mesh tally was used to determine nuclear heating, with a 3 mm mesh resolution over the FWS module. The results were interpolated onto a high-fidelity tetrahedral mesh for use in CFD analysis. Nuclear heating distribution in the FW layers is shown in Fig. 6. The interpolated nuclear heating results were used by Ying and Narula in CFD analysis to determine the temperature distribution [15]. DAG-MCNP is routinely used to perform such analyses of modified ITER FWS designs.

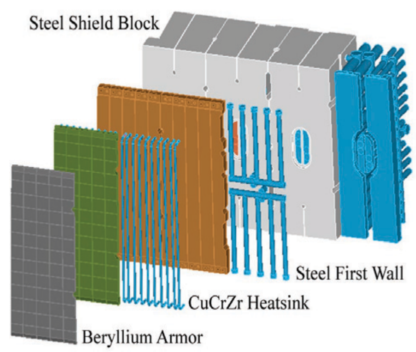

Figure 5. CAD geometry of recent FWS module design.

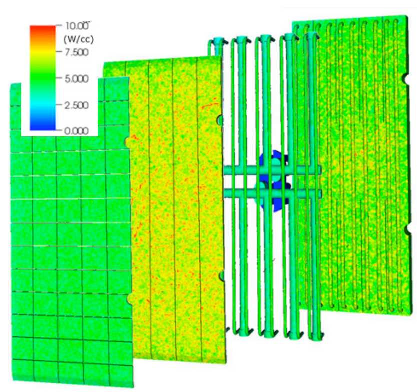

Figure 6. FW nuclear heating results.

V. 3-D ANALYSIS OF ITER DCLL TBM

In support of the ITER Test Blanket Module (TBM) program, the US has been developing a TBM design based on the dual coolant lead lithium (DCLL) blanket concept [10]. The basic idea of the DCLL blanket is to use helium to remove all heat deposited in the FW and blanket structure, and a flowing, self-cooled, lead lithium (PbLi) breeder to remove nuclear heat generated in the breeding zone at a high temperature for efficient power conversion [10]. This is the preferred US blanket concept for commercial fusion plants. Each PbLi channel is lined with a SiC flow channel insert (FCI) that separates the PbLi from the RAFS structure. This FCI performs two important functions: (a) the FCI thermally insulates the PbLi so that its temperature can be considerably higher than the surrounding structure, and (b) the FCI also provides electrical insulation between the PbLi flow and the thick, load-bearing RAFS walls to reduce the MHD pressure drop to a manageable level, even in high magnetic field regions. The concept will be tested in one half of a designated test port where it will be mounted inside a water-cooled frame designed to hold two different test modules. The design has been evolving over the past several years following several technical reviews and it converged on a reference design for which detailed CAD models were generated. Significant heterogeneity exists in the module as shown in Fig. 7 for the mid-plane section. In addition, the material configuration inside the TBM varies significantly in the vertical direction. To account for these geometrical details, we used DAG-MCNP to perform 3-D nuclear analysis of the TBM [16].

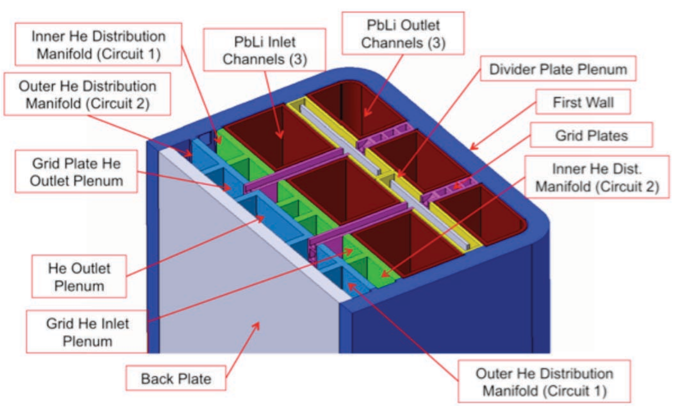

Figure 7. Configuration at mid-plane of TBM.

Helium in the model was represented by void. A full PbLi volume has been created for analysis. A simplified CAD model with homogenized zones was generated for the frame. The CAD model for the DCLL TBM was inserted in the CAD model for the frame and the integrated model was used in the analysis. The calculations were performed in steps. In the first step, the CAD model based on a 40° sector of the ITER benchmark was used along with the detailed ITER source to generate a surface source in front of the integrated frame/TBM model. This surface source was used in a subsequent calculation with half of the frame with a TBM inserted in it and surrounded with reflecting boundaries. Detailed mesh tallies of nuclear heating, radiation damage, and tritium production were generated over the TBM. Fig. 8 shows distribution of nuclear heating at mid-plane. Total nuclear heating in the TBM is 0.374 MW. It is interesting to note that this is 35% lower than that estimated based on 1-D models [17]. This is due to exact modeling of heterogeneity and surrounding massive water-cooled frame and accurate representation of the exact source and contribution from other in-vessel components. Tritium generation rate in the PbLi is 4.19×10^{-7} g/s during a D-T pulse with 500 MW fusion power which is ~45% lower than the value obtained from 1-D estimate. Fig. 9 gives radiation damage parameters at a vertical cross section in the module. Peak radiation damage parameters are 10-30% lower than the 1-D estimates.

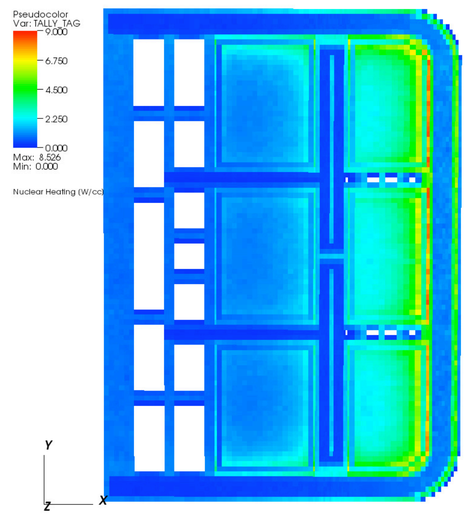

Figure 8. Nuclear heating (W/cm^3) at mid-plane of TBM.

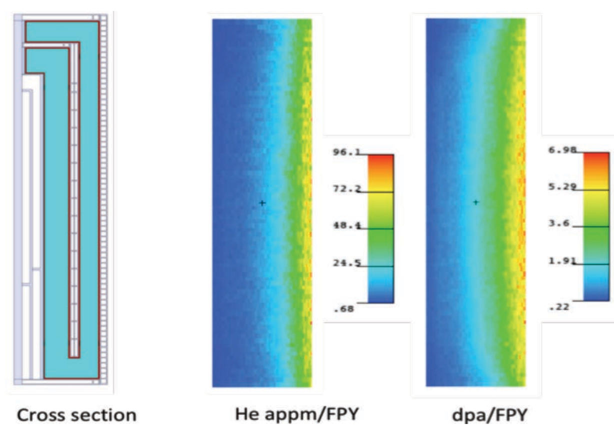

Figure 9. Steel damage parameters at vertical section of TBM.

VI. 3-D ANALYSIS FOR ARIES-CS

DAG-MCNP was used to perform 3-D nuclear analysis of the compact stellarator conceptual design ARIES-CS [18]. Nuclear analysis for such a configuration is challenging due to the complex stellarator helical configuration with FW shape changing in both poloidal and toroidal directions. In addition, the source profile is complex with significant variation of the plasma shape as one moves toroidally within a 120 degree field period. Tools that handle only simple 2nd order surfaces will require significant geometrical approximations. Hence, DAG-MCNP is the only tool suited for such helical systems.

A model of the full ARIES-CS system was developed for the 3-D neutronics calculations. The primary goals of this analysis were to determine the tritium breeding ratio (TBR) and neutron energy multiplication (M_n) for the DCLL blanket in the complex ARIES-CS geometric configuration. The solid model was generated with blanket, shield, manifold, and divertors as shown in Fig. 10. The neutron wall loading (un-collided neutron current) distribution was calculated within a field period and contour maps are given in Fig. 11 for a scrape-off layer of 5 cm [18].

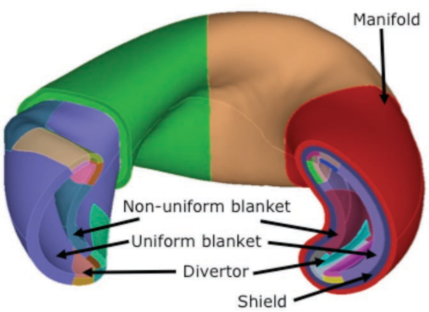

Figure 10. ARIES-CS chamber CAD model.

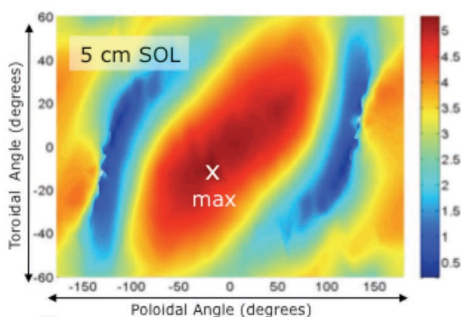

Figure 11. Map of neutron wall loading (MW/m^2) within a field period.

The results for the TBR and M_n were determined for each major component and for the whole device [18]. The target TBR of 1.1 is achieved with a ^{6}Li enrichment of at least 65%. The majority (>77%) of tritium breeding occurs in the uniform blanket region and approximately 2.5% occurs in the blanket region behind the divertor. The energy multiplication is 1.16 and was found to be independent of the ^{6}Li enrichment, Approximately half of the nuclear heating is from gamma photons and the majority of nuclear heating is produced in the blanket with only ~10% generated in the divertor and shield.

VII. Nuclear Analysis of Laser Fusion Final Optics

The High Average Power Laser (HAPL) program aims at developing laser inertial fusion energy based on direct drive targets and a dry wall chamber [8]. Power plant designs were assessed with targets driven by forty KrF laser beams. The final optics system that focuses the laser onto the target includes grazing incidence metallic mirrors (GIMM) located at 24 m from the target. The GIMM is used to protect the dielectric mirrors that are placed out of the direct line-of-sight of the target from neutron damage. However, secondary neutrons resulting from interactions of the streaming source neutrons with the GIMM and the biological shield can result in significant flux at the dielectric mirrors. Neutron traps are utilized in the shield behind the GIMM. Radiation environment at the GIMM is determined primarily by the direct un-collided neutrons emanating from the target. The nuclear environment at the dielectric mirrors is impacted by the GIMM material and the shielding geometrical configuration. Fig. 12 gives a CAD model for one of the 40 beam lines with associated optics. The focusing dielectric mirror (M2) is located at 14.9 m from the center of the GIMM (M1) and a plane dielectric turning mirror (M3) is at 1.6-6 m from M2.

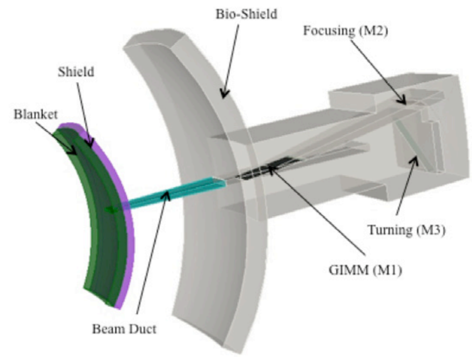

Figure 12. 3-D model for final optics fully surrounded by biological shield

We utilized DAG-MCNP to perform nuclear analysis for the HAPL final optics system using the CAD model shown in Fig. 12 with surrounding planar reflective boundaries [19]. We assessed the impact of the GIMM material on neutron streaming and nuclear environment at the dielectric final optics. Options considered for the GIMM substrate material included SiC and the Al alloys AlBeMet162 and Al-6061. The results indicated that the fast neutron flux at the dielectric optics depends on the material choice for the GIMM and the total GIMM areal density and increases as the total areal density of the GIMM increases [19]. The AlBeMet GIMM results in the highest flux level (~60% higher) due to neutron multiplication in the beryllium and the larger thickness required for stiffness. The fast neutron flux decreases by about two orders of magnitude as one moves from the GIMM to the focusing mirror with an additional two orders of magnitude attenuation at the turning mirror accompanied with significant spectrum softening [19].

We investigated also the effect of shielding geometrical configurations on the nuclear environment at the dielectric mirrors. Although the configuration in Fig. 12 reduces the volume that should be maintained under vacuum, provides good support for the GIMM and eliminates streaming contribution from adjacent ports, it requires adding concrete shielding to fully enclose the GIMMs and associated dielectric mirrors in the 40 laser beam penetrations. There was also a concern that this configuration could lead to steering the streaming neutrons towards the sensitive dielectric mirrors. Using DAG-MCNP with direct coupling to CAD models allowed us to quickly assess other configuration options [20].

We utilized the mesh tally capability of DAG-MCNP to generate a high-resolution map of the fast neutron flux along the beam line for three shielding configurations [20]. The fast neutron (E>0.1 MeV) flux results are shown in Fig. 13. In option I, the flux is high along the beam line penetration but drops rapidly around it due to shielding by the surrounding biological shield. It is clear that in the open configurations II and III, the flux is relatively high in the space between the chamber and biological shield due to contribution from neutrons streaming through all 40 beam ports in the chamber. This flux is slightly reduced in option III due to partial trapping of streaming neutrons in the added neutron traps. The higher fluxes in the open configurations result in higher fluxes at the dielectric mirrors. Based on this analysis, the initial shield configuration was selected for the baseline HAPL design.

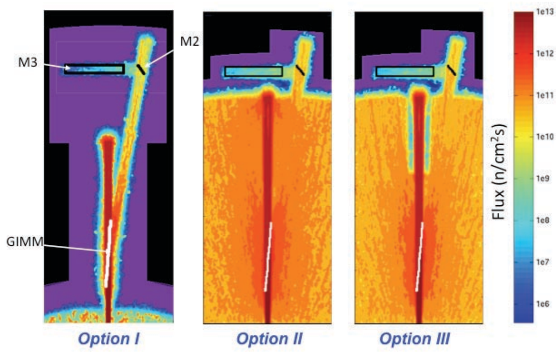

Figure 13. Fast neutron flux distribution for three shielding configurations.

VIII. Summary and Conclusions

An innovative computational tool (DAG-MCNP) has been developed for efficient and accurate 3-D nuclear analysis of geometrically complex fusion systems. It permits direct use of CAD-based solid models, preserves the geometrical details without simplification, eliminates possible human error in modeling, and allows faster design iterations. Most features of the standard MCNP are now supported in the DAG-MCNP software with an added feature of allocating materials with densities and defining tallies and boundary conditions in the solid model geometry file itself that reduces the burden on the user. The tool has been successfully validated using an ITER benchmark problem. DAG-MCNP has been applied to perform 3-D nuclear analysis for several fusion designs including the ARIES Compact Stellarator (ARIES-CS), the High Average Power Laser (HAPL) inertial fusion power plant, ITER first wall/shield (FWS) modules, and the ITER dual coolant lithium lead test blanket module (TBM). Highlights of these analyses presented here demonstrate the capability of that innovative tool in generating high-fidelity high-resolution results that provide great help to the design process of geometrically complex fusion systems with high degree of heterogeneity. DAG-MCNP is used routinely for efficient and fast design iterations. This tool will be the core for a full CAD-based simulation predictive capability that directly couples engineering analyses directly to the CAD solid model.

Acknowledgment

Funding was provided through grants from the US DOE.

References

[1] H. Tsige-Tamirat, U. Fischer, A. Serikov, and S. Stickel, “Use of McCad for the conversion of ITER CAD data to MCNP geometry,” Fusion Engineering and Design, vol. 83, p. 1771 (2008).

[2] Y. Li, L. Lu, A. Ding, H. Hu, Q. Zeng, S. Zheng, and Y. Wu, “Benchmarking of MCAM 4.0 with the ITER 3D model,” Fusion Engineering and Design, vol. 82, p. 2861 (2007).

[3] X-5 Monte Carlo Team, “MCNP-A General Monte Carlo N-Particle Transport Code, Version 5-Volume II: Users Guide,” LA-CP-03-0245, Los Alamos National Laboratory (April 2003, revised 2/1/2008).

[4] M. Wang, T.J. Tautges, and D. Henderson, “Acceleration of direct-interface cad-based Monte Carlo radiation transport,” American Nuclear Society's 14th Biennial Topical Meeting of the Radiation Protection and Shielding Division, La Grange Park, United States: American Nuclear Society, 2006, pp. 50-53.

[5] T. Tautges, P.P.H. Wilson, J. Kraftcheck, B. Smith, and D. Henderson, “Acceleration Techniques for Direct Use of CAD-Based Geometries in Monte Carlo Radiation Transport,” Proceedings of International Conference on Mathematics, Computational Methods & Reactor Physics (M&C 2009), Saratoga Springs, New York, May 3-7, 2009.

[6] P. Wilson, et al., “State of the Art 3-D Radiation Transport Methods for Fusion Energy Systems,” Fusion Engineering and Design, vol. 83, pp. 824-833 (2008).

[7] F. Najmabadi, A.R. Raffray, and ARIES-CS Team, “The ARIES-CS Compact Stellarator Fusion Power Plant,” Fusion Sci. Technol., vol. 54, pp. 655-672 (2008).

[8] J. Sethian, et al., “An Overview of the Development of the First Wall and Other Principal Components of a Laser Fusion Power Plant,” J. Nucl. Mater., vol. 347, pp. 161-177 (2005).

[9] ITER Design Description Document, 1.6 Blanket, ITER Document ITER_D_22F3M6 v2.0, August 2004.

[10] C.P.C. Wong, S. Malang, M. Sawan, M. Dagher, S. Smolentsev, B. Merrill, et al., “An overview of dual coolant Pb–17Li breeder first wall and blanket concept development for the US ITER-TBM design,” Fusion Engineering & Design, vol. 81, pp. 461-467 (2006).

[11] T.J. Tautges, R. Meyers, K. Merkley, C. Stimpson, and C. Ernst, MOAB: A Mesh-Oriented Database, Sandia National Laboratories, 2004.

[12] T.J. Tautges, “CGM: A geometry interface for mesh generation, analysis and other applications,” Engineering with Computers, vol. 17, pp. 299-314 (2001).

[13] B. Smith, P. Wilson, and M.E. Sawan, “Three Dimensional Neutronics Analysis of the ITER First Wall/Shield Module 13,” Proceedings of the 22nd IEEE/NPSS Symposium on Fusion Engineering (SOFE), 17-21 June 2007, Albuquerque NM, IEEE Cat. No. 07CH37901C.

[14] B. Smith, P. Wilson, M. Sawan, and T. Bohm, “Source Profile Analysis for the ITER First Wall/Shield Module 13,” Fusion Science & Technology, in press.

[15] Alice Ying, University of California-Los Angeles, personal communication, 2008.

[16] M.E. Sawan, B. Smith, E.P. Marriott, and P.P.H. Wilson, “Three-Dimensional Nuclear Analysis for the US Dual Coolant Lithium Lead ITER Test Blanket Module,” Fusion Engineering & Design, in press.

[17] M. Sawan, E. Marriott, and M. Dagher, “Neutronics Performance Parameters for the US Dual Coolant Lead Lithium ITER Test Blanket Module,” these proceedings.

[18] L. El-Guebaly, P. Wilson, D. Henderson, M. Sawan, G. Sviatoslavsky, T. Tautges et al., “Designing ARIES-CS Compact Radial Build and Nuclear System: Neutronics, Shielding, and Activation,” Fusion Science and Technology, vol. 54/3, pp. 747-770 (2008).

[19] M. Sawan, M. McGeoch, A. Ibrahim, and P. Wilson, “Nuclear Assessment of Final Optics of a KrF Laser Driven Fusion Power Plant,” Fusion Science & Technology, vol. 52/4, pp. 938-942 (2007).

[20] M. Sawan, A. Ibrahim, T.D. Bohm, and P. Wilson, “3-D Nuclear Analysis of the Final Optics of a Laser Driven Fusion Power Plant,” Fusion Engineering & Design, vol. 83, pp. 1879-1883 (2008).